ISTITUTO NAZIONALE DI FISICA NUCLEARE
Laboratori Nazionali di Frascati

ECFA/LEP Working Group
SSG/6/2/March 1979

LNF-79/23(R)
18 Aprile 1979

R. Del Fabbro and G. P. Murtas: TAGGING SYSTEMS AT LEP "SHORT INSERTION": ANGULAR ACCEPTANCES AND EFFICIENCIES.

Servizio Documentazione
dei Laboratori Nazionali di Frascati
Cas. Postale 13 - Frascati (Roma)

ECFA/LEP Working Group
SSG/6/2/March 1979

INFN - Laboratori Nazionali di Frascati
Servizio Documentazione

LNF-79/23(R)
18 Aprile 1979

R. Del Fabbro[x] and G. P. Murtas: TAGGING SYSTEMS AT LEP "SHORT INSERTION": ANGULAR ACCEPTANCES AND EFFICIENCIES.

1. - INTRODUCTION.

We have performed a preliminary study in order to investigate on the real possibility to set up a tagging detector at LEP.

Actually some preliminary work has been done on this subject[1-5]. As far as the two different "insertions" of the storage ring are concerned, the long insertion (the lower luminosity) is more suitable for the two photons physics studies[6]. Indeed there is no problem for a good efficiency tagging device in front to the quadrupole Q1, reaching a minimum electron angle as small as ~ 10 mrad. On the contrary in the short insertion ($\pm$ 5 m) the minimum electron angle is at least doubled. However in the short insertion case one can think of a tagging device placed between the quadrupole Q11 and Q12 and exploring the electron angular region from 1-4 mrad to ~ 25 mrad.

We have investigated the tagging possibility for the short insertion case thinking of two devices: in front (and possibly around) and behind the quadrupole Q11.

Three different cases for the quadrupole Q11 (see the particular in Fig. 6) have been considered: the standard hyperbolic quadrupole, the Panofsky quadrupole with rectangular aperture and current shaped field[3] and the "slim" superconducting quadrupole[7] with the field shaped by coils located around a circular aperture. The outer transverse dimensions of the "slim" quadrupole are about twice as small as those of the standard quadrupole, while the length and the magnetic parameters are identical.

2. - TAGGING IN FRONT TO THE QUADRUPOLE Q11.

An ideal tagging device in front to the quadrupole Q11 could cover an electron minimum angle θ_{min} of 12 mrad, but it has been evaluated[3] that, if one takes in account the detector size, the counter edges, the shielding and so on, 22 mrad are more realistic.

The single tagging efficiency can be defined as the ratio between the flux of the tagging electron of energy X_e (in beam energy unit) emitted between the angles θ_{min} and θ_{max} and the total flux emitted in the whole angular range $0 - \pi$.

(x) - Istituto Nazionale di Fisica Nucleare, Sezione di Pisa.

The electron flux emitted between the angles θ_{min} and θ_{max} according to the "Equivalent Photon Approximation" can be written:

$$N(X_e, \theta_{min}, \theta_{max}) = \frac{\alpha}{\pi(1-X_e)} \left[(1+X_e^2) \ln \frac{\theta_{max}}{\theta_{min}} - \frac{(1+X_e)^2}{4} \ln \frac{(1-X_e)^2 + X_e \theta_{max}^2}{(1-X_e)^2 + X_e \theta_{min}^2} \right] \quad (1)$$

and the total flux:

$$N(X_e) = \frac{\alpha}{\pi(1-X_e)} \left[(1+X_e^2) \left(\ln \frac{E}{m_e} - \frac{1}{2} \right) + \frac{(1-X_e)^2}{2} \left(\ln \frac{2X_e}{1-X_e} + 1 \right) + \frac{(1+X_e)^2}{2} \ln \frac{2X_e}{1+X_e} \right] \quad (2)$$

where E is the beam energy and m_e the electron mass.

The ratio of the expressions (1) and (2) integrated in the electron energy X_e from zero to X_{emax} represents the efficiency $\varepsilon_{st}(X_{emax}, \theta_{min}, \theta_{max})$ of the single tagging device for the electron energies up to X_{emax}.

Since the leading term of the expression (1) is $\ln(\theta_{max}/\theta_{min})$ and that of the expression (2) is $\ln(E/m_e)$, a rough evaluation of the tagging efficiency is:

$$\frac{\ln \frac{\theta_{max}}{\theta_{min}}}{\ln \frac{E}{m_e}} .$$

In the Fig. 1 we show the behaviour of the tagging efficiency versus X_{emax}. The two curves shown in Fig. 1 labelled (22-110 mrad) and (22-55 mrad) refer to a tagging placed in front to and not exceeding the quadrupole cross section in the case of the standard and "slim" quadrupole respectively, the third curve labelled (22-300 mrad) refers to a tagging in front to the quadrupole and eventually around the quadrupole reaching a maximum electron angle of 300 mrad.

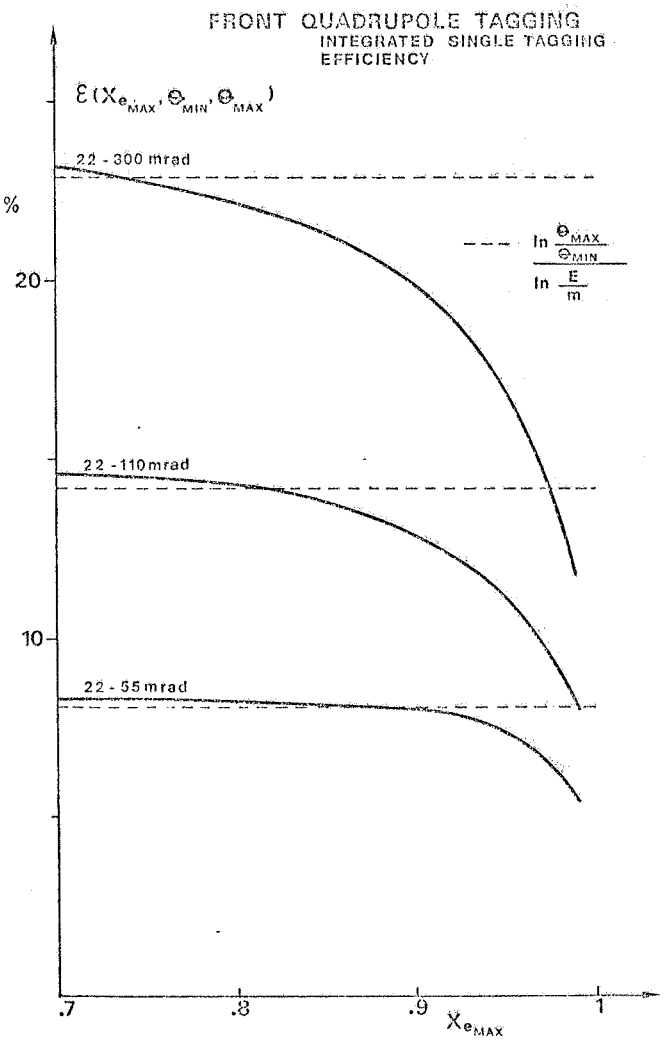

FIG. 1 - Integrated single tagging efficiency of the front quadrupole tagging versus the maximum integration limit.

3. - TAGGING BEHIND THE QUADRUPOLE Q11.

We have studied this case considering the trajectories of electrons emitted from the crossing point at the energy X_e with a polar and azimuthal angles θ and ϕ of emission and running through the optical components of the machine close to the experimental intersection region (see Fig. 2a).

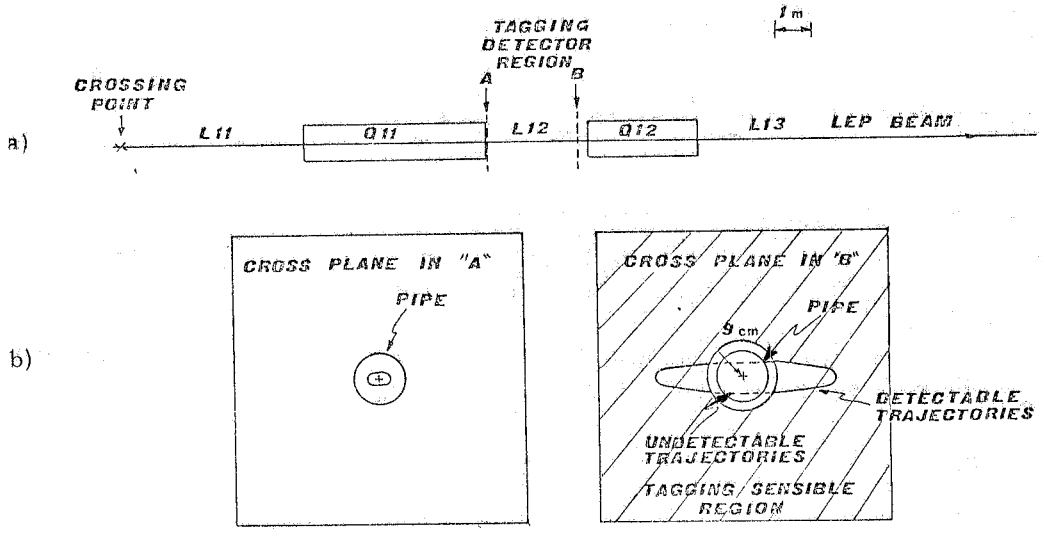

FIG. 2 - a) Outline of the half environment of the short insertion; b) Intersection patterns of the electron trajectories at fixed energy and polar angle and for all values of the azimuthal angle on the cross planes placed in the positions "A" and "B"; visible evidence of both detectable and undetectable trajectories is given.

In our investigation we don't think of any particular detector, but only we consider as "detectable" any electron which reaches the end of the quadrupole Q11 having not hit thick material and crosses the pipe along a range of 2.5 meters far from the quadrupole end, up to a minimum distance of 9 cm from the circulating beam accounting for the pipe size and the detector edge.

In the Fig. 2b the pattern of the crossing points of a family of trajectories at fixed X_e and θ values and for all values of ϕ with a transversal plane placed in the positions A and B are shown. So we can say what fraction of trajectories can satisfy the condition of "to be detectable".

This fraction (in percent) is given in Fig. 3 versus the angle θ for four values of the electron energy in the standard quadrupole case. At threshold the fraction of the "detectable" trajec-

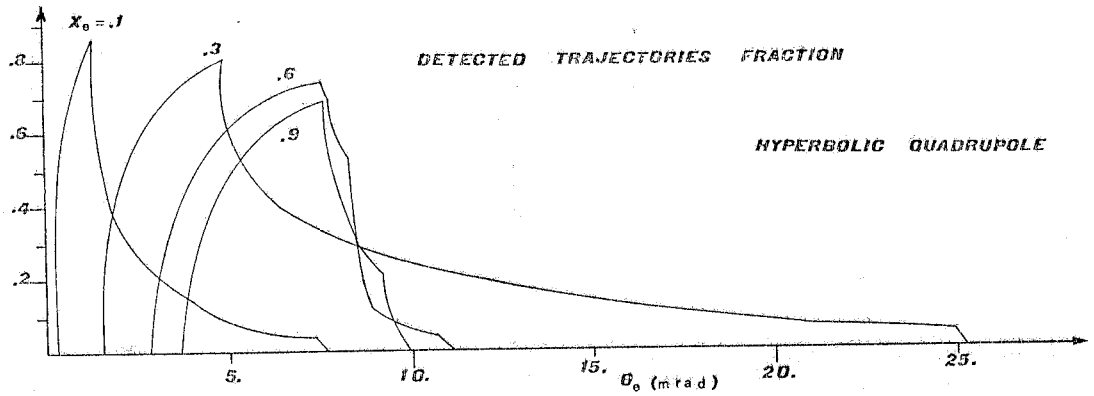

FIG. 3 - Detected trajectories fraction distribution versus the electron polar angle and for various electron energies for the standard quadrupole case.

tories is high, but it falls quickly as the angle θ increases, because the radial component is washed away very soon by the defocusing action of the quadrupole.

The maximum value, where the fraction vanishes, corresponds to the condition when all trajectories hit the poles ; this condition is, of course, energy dependent.

In the Fig. 4 curves are shown for the Panofsky quadrupole, where we have considered a rectangular gap section 60×16 cm^2.

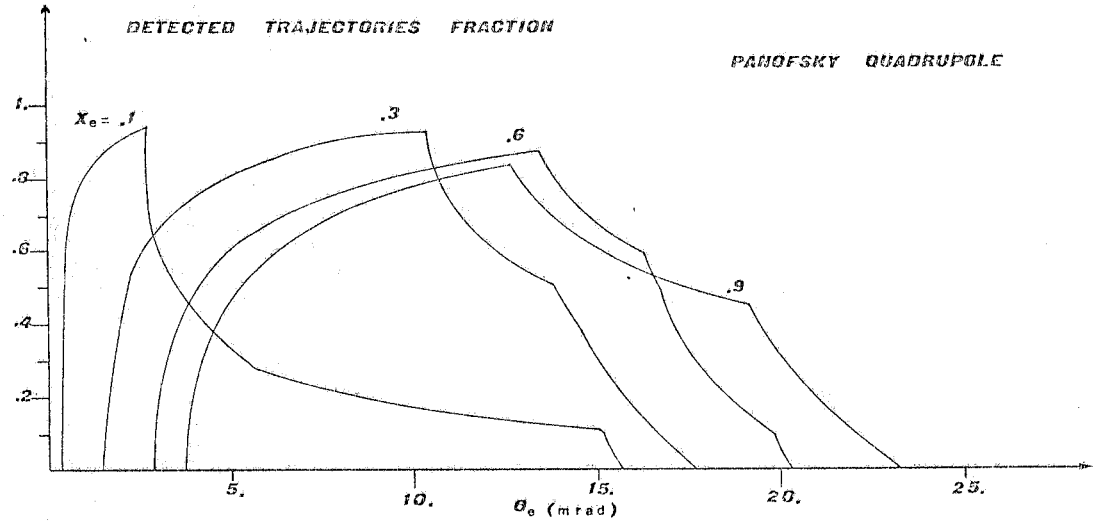

FIG. 4 - Detected trajectories fraction distribution versus the electron polar angle and for various electron energies for the Panofsky quadrupole case.

The range of θ where the fraction is nonzero is larger than the standard quadrupole case. Moreover the trajectories fraction is somewhat higher and falls slowly owing to the gap is much larger than the previous one in the radial direction.

In the Fig. 5 the minimum and maximum angle of the θ range are shown versus the electron energy X_e ; the minimum curve is obviously common to the considered cases ; on the contrary the θ_{max} curves look different because are strongly gap dependent. At low energy the curve θ_{max} of the standard quadrupole is higher than the corresponding curve of the Panofsky quadrupole because in that energy region the trajectories oscillate in the vertical direction (quadrupole focusing action) and the standard quadrupole having a larger vertical gap gets a larger acceptance. Besides we note that in the standard quadrupole case,

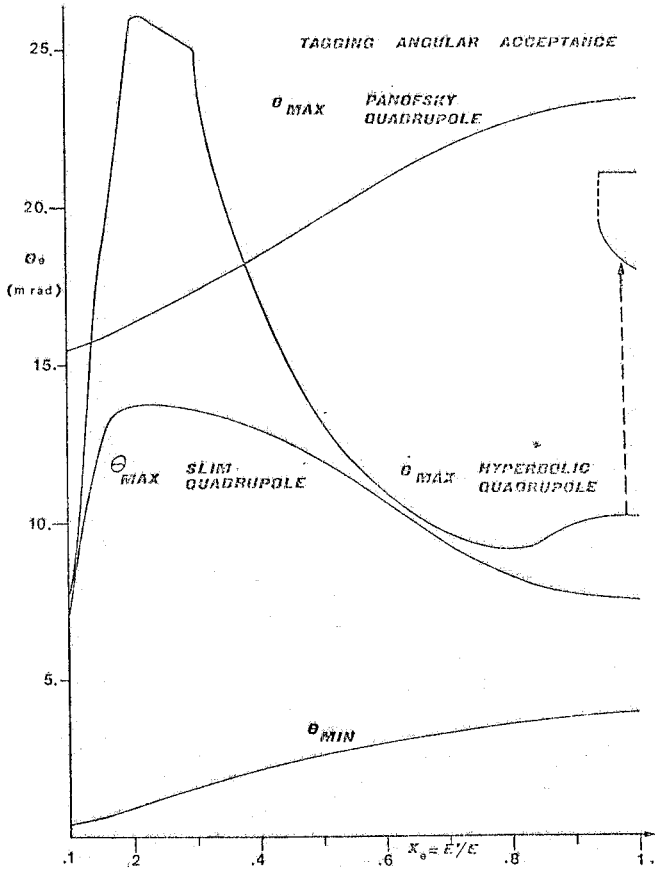

FIG. 5 - Electron angular acceptance distributions of a tagging device placed behind the quadrupole Q11 versus the electron energy for different quadrupole cases. θ_{min} distribution is common for all cases.

at high electron energy, trajectories with azimuthal ϕ angle near 0 and π are detected; however a separate region exists, where trajectories with azimuthal angle very close to $\pi/2$ and $3/2\pi$ can be detected too, only if the polar angle θ is as large as $\sim$ 20 mrad for escaping pipe requirement.

In order to get the tagging efficiency we need to do some considerations. The nonleading term of the expression (1) is at least two order of magnitude smaller than the leading term up to the value $X_e = 0.9$; form 0.9 to 0.98 the nonleading term is not larger than 20%, taking in account that behind the quadrupole $2 < \theta < 20$ mrad, so in that approximation we write the ratio:

$$\varepsilon_{st} = \frac{\ln(\theta_{max}/\theta_{min})}{\ln\frac{E}{m_e} - \frac{1}{2} + \frac{(1+X_e)^2}{2(1+X_e^2)}\left(\ln\frac{2X_e}{1-X_e}+1\right) + \frac{(1+X_e)^2}{2(1+X_e^2)}\ln\frac{2X_e}{1+X_e}} = \frac{\ln(\theta_{max}/\theta_{min})}{F(X_e, E)} \qquad (3)$$

This ratio might express the right efficiency if all electrons emitted between θ_{min} and θ_{max} were effectively detected. But this is not our case because only a fraction are detected depending on X_e, θ and ϕ. So in order to evaluate the right efficiency we can operate in the following way: for a fixed electron energy we can divide the angular range $\theta_{min} \div \theta_{max}$ in N parts, i.e. we can write:

$$\ln\frac{\theta_{max}}{\theta_{min}} = \ln\left[\frac{\theta_{max}}{\theta_2}\,\frac{\theta_2}{\theta_3}\,\cdots\,\frac{\theta_{N-2}}{\theta_{N-1}}\,\frac{\theta_{N-1}}{\theta_{min}}\right] = \sum_{i=2}^{N}\ln\frac{\theta_{i-1}}{\theta_i} \qquad (4)$$

where $\theta_{max} = \theta_1$ and $\theta_{min} = \theta_N$. So the expression (3) can be written in the form:

$$\varepsilon_{st}(X_e) = \sum_{i=2}^{N}\varepsilon_i \qquad (5)$$

where:

$$\varepsilon_i = \frac{\ln\frac{\theta_{i-1}}{\theta_i}}{F(X_e, E)} \,.$$

Now if we choose the θ_{i-1}, θ_i couples in such a way that the fraction f_i of the detectable electrons is practically constant for the θ values in the range $\theta_{i-1} \div \theta_i$, then we can express the effective efficiency with the formula:

$$\varepsilon_{st} = \sum_{i=2}^{N}\varepsilon_i f_i \,. \qquad (6)$$

In the Fig. 6 the effective efficiencies are shown versus the electron energy; they are corresponding to the Panofsky quadrupole, the standard quadrupole and the "slim" quadrupole.

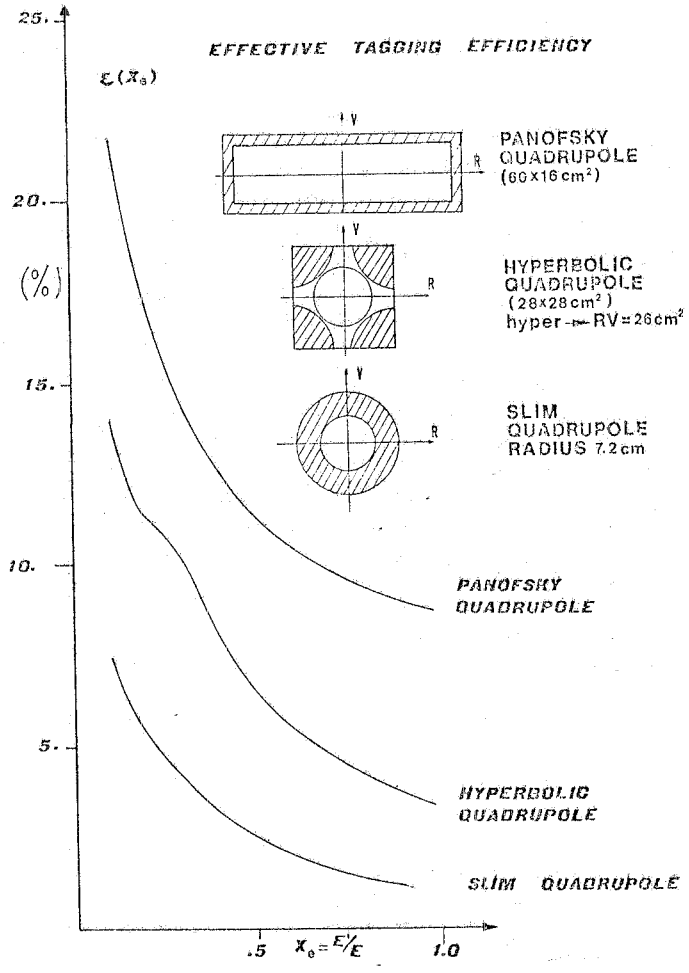

FIG. 6 - Effective tagging efficiency distributions of a tagging device placed behind the quadrupole Q11 versus the electron energy for different quadrupole cases. In the particular: sizes and geometrical data of the considered quadrupoles.

We remark that by the Panofsky quadrupole one gets a factor of two in respect to the standard quadrupole.

At last we give in Table I the integrated values of the efficiencies, i.e. :

$$\frac{\int_{0.1}^{0.95} dX_e N(X_e)\, \varepsilon_{st}(X_e)}{\int_{0.1}^{0.95} dX_e N(X_e)}$$

weighted on the electron energy spectrum in the range 0.1÷0.95.

TABLE I

Quadrupole	Weighted efficiency (%)
Panofsky	10
Standard	5.5
Slim	1.8

4. - REAL ELECTRON BEAM EFFECT ON THE TAGGING EFFICIENCY.

So far we have performed our analysis on the efficiency and the angular acceptance of a tagging system in the hypothesis of an ideal electron beam circulating on the synchronous particle orbit with a zero emittance.

The aim of this section is to evaluate the effect of a real electron beam on the tagging efficiency.

For this purpose we report in Table II the given[8] radial and vertical standard deviations for both spacial and angular spread of the LEP beam in the short insertion cross point, due both to the beam emittance and to the systematic errors induced by some possible misalignments of the optical components of the machine.

TABLE II

LEP beam spatial and angular standard deviations in the short insertion cross point.

Errors	Coordinate (mm) vertical	radial	Angle (mrad) vertical	radial
Systematic	0.2	0.6	2.	0.38
Statistic	0.02	0.32	0.2	0.2

In view of the effect we are searching for, the examination of the Table II shows that the most important parameter is the angular spread, because it implies both a variation of the trajectory derivative and a spatial displacement at the quadrupole Q11 input.

Moreover the spatial spread is of the order of a fraction of millimeter, on the contrary the angular spread produces at the quadrupole input a displacement of a few millimeters.

For this reason we think that it is better at first to look at the angular spread effect.

We also skip the trivial case of the tagging in front to the quadrupole Q11 and we focalize our interest on the tagging behind the quadrupole.

Following this trend we have considered an electron beam at a fixed energy and emitted from a point-like source in the cross point and affected by a vertical or radial angular deviation in respect to the optical axis of the machine. Thus we have studied the corresponding effect on the tagging efficiency in the range from 0.5 to 2 mrad of the deviation angle α.

We have choosen the quadrupole Q11 as the Panofsky quadrupole, since it turns out to get the best efficiency. On the other hand, if necessary, we don't find any difficulty to extend in the next step our analysis to other types of quadrupoles.

Now if the electron beam suffers for a vertical or radial angular deviation in the cross point, then the pattern of the trajectories family at various ϑ values and for all values of ϕ at the

input of the quadrupole Q11 look like those shown in Figs. 7a) and b) respectively.

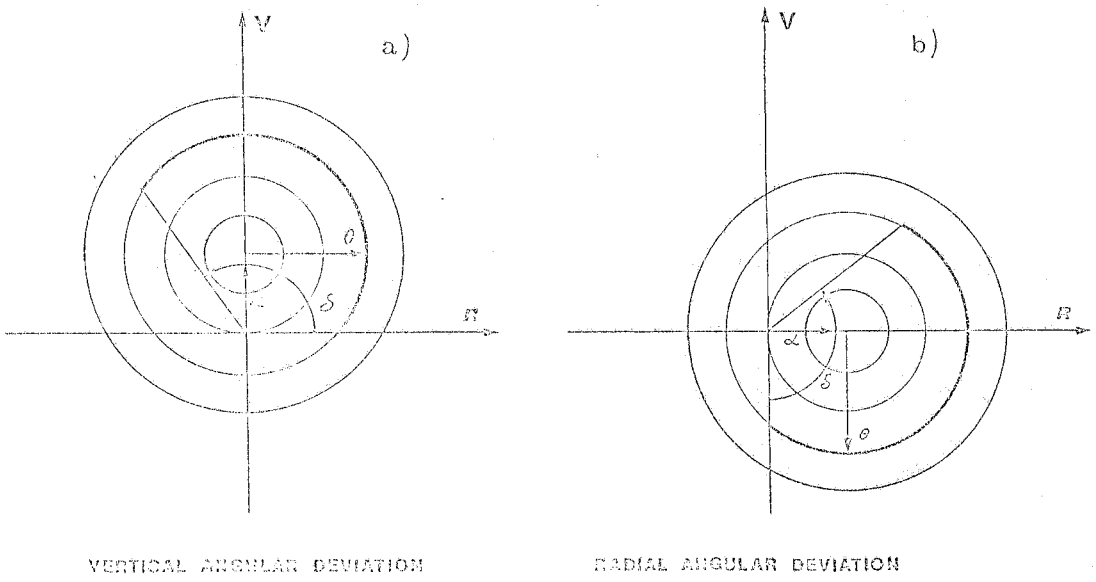

FIG. 7 - Intersection patterns of a vertically (side "a") and radially (side "b") deviated electron beam of an angle α with a crossing plane at input of the quadrupole Q11.

Of course the deviation α introduces an asymmetry between the emitted trajectories and the tagging system.

In fact for a fixed θ value the number u of the trajectories relative to the azimuthal angle δ in the range $0 \rightarrow \pi$ (see Fig. 7) will be different from the number w relative to the range $\pi \rightarrow 2\pi$. Now if we indicate by u' and w' the amount of the detected trajectories, then the detected trajectories fraction rules out to be: u'/u and w'/w.

In the Fig. 8 we show three distributions of the detected trajectories fraction versus the angle θ for a fixed electron energy and correspondently for the following values of the vertical deviation angle α of 0.5, 1 and 2 mrad.

In the Fig. 9 similar distributions are shown relative to a radial deviation of the electron beam.

In the Figs. 8 and 9 the curve relative to $\alpha = 0$ is shown for comparison. Let us now to analyse the shape of this curve corresponding to an ideal electron beam: it rises fast at thershold up to a high value, which is got in plateau up to the value θ_r, where the curve decreases with a well defined slope. That decrement corresponds to losses of trajectories around the radial plane. At the value θ_v the curve changes more fastly his slope; this point corresponds to further losses of trajectories around the vertical plane. Now we can see in Figs. 8 and 9 how the beam angular deviation produces a distorsion of the curve correspondently to his asymmetric position: in Fig. 8 we observe that the value θ_r doesn't change for the different curves, since the beam is still radially symmetric, but θ_v changes of the amount $\pm\alpha$; conversely in Fig. 9 the value θ_r changes of the amount $\pm\alpha$, but θ_v doesn't change, how should be, because the beam is vertically symmetric.

As far as the threshold and the rising behaviour are concerned, they look different in the radial and vertical deviation cases; however we remark that those behaviours can be predicted analytically.

We have performed these calculations and we have found a perfect agreement with the results of the computing program.

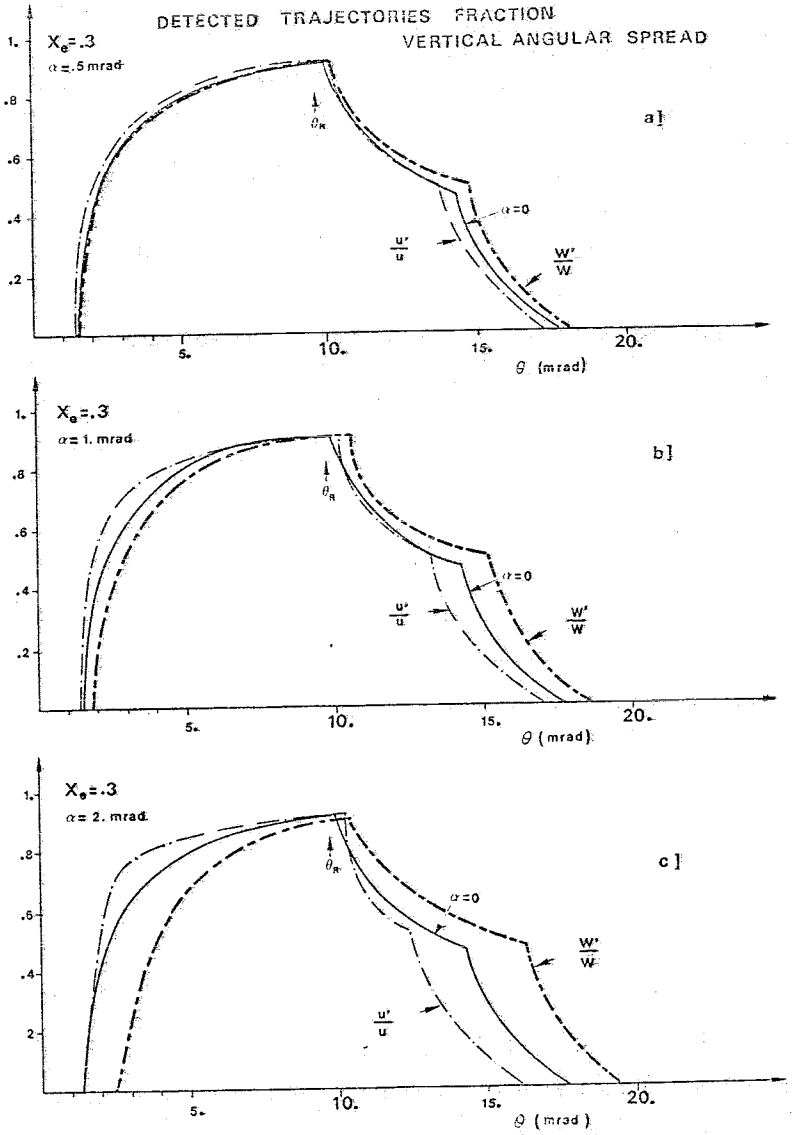

FIG. 8 - Detected trajectories fraction distributions versus the electron polar angle of a vertically deviated electron beam of energy X_e=0.3. a), b) and c) distributions refer to an angular deviation α of 0.5, 1 and 2 mrad. The quadrupole Q11 considered is the Panofsky quadrupole.

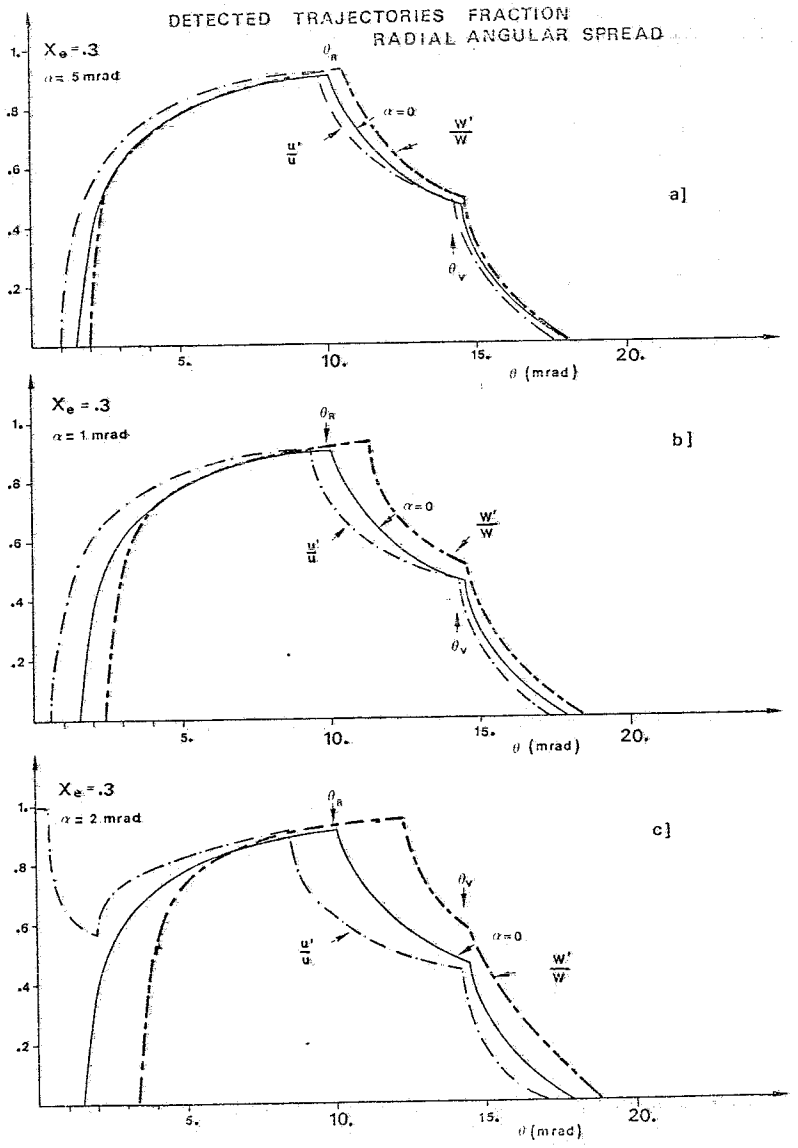

FIG. 9 - Detected trajectories fraction distributions versus the electron polar angle of a radially deviated electron beam of energy X_e=0.3. a), b) and c) distributions refer to an angular deviation α of 0.5, 1 and 2 mrad. The quadrupole Q11 considered is the Panofsky quadrupole.

In Fig. 10 we report the tagging effective efficiencies for the evaluated angular deviations ; calculations have been performed how previously described for the ideal case, however the distributions u'/u and w'/w have been averaged with the corresponding weights u/(u+w) and w/(u+w).

Apart the low energy region, where the photon-photon cross section is considerably small, the vertical deviation of the electron beam doesn't seem to produce any relevant effect. So the result of this analysis lead us to affirm that both spatial and angular spread of the electron beam, as given in Table II, doesn't generate any important change on the tagging efficiency of the short insertion.

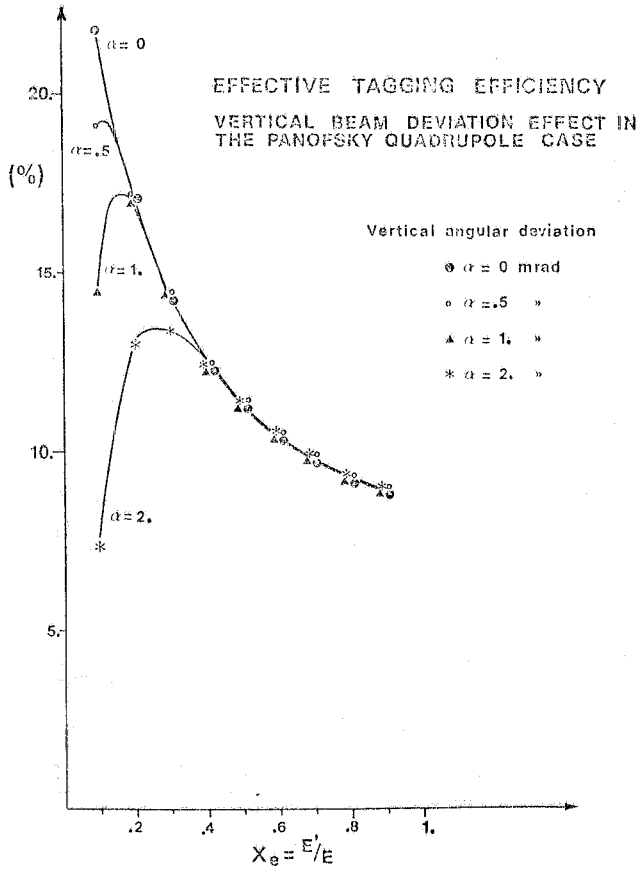

FIG. 10 - Effective tagging efficiency distribution versus the electron energy of a tagging device placed behind the Panofsky quadrupole for 0, 0.5, 1 and 2 mrad vertical angular deviations of the electron beam.

5. - CONCLUSIONS.

Our results obtained using the machine data given in the LEP-Note-121 at the beam energy of 80 GeV are summarized in Table III for the considered tagging devices in front, around and behind the quadrupole Q11.

In Table III the different cases in using the standard, the Panofsky and the "slim" quadrupole are considered. All efficiencies refer to the whole electron energy spectrum up to the value $X_e = 0.95$.

TABLE III

Quadrupole	Tagging system	covered angles (mrad)	efficiency (%)
standard quadrupole	behind the quadrupole	2÷4 - 10	5.5
	in front to the quadrupole	22 - 110	11
	in front and around the quadr.	22 - 300	17
Panofsky quadrupole	behind the quadrupole	2÷4 - 22	10
	in front to the quadrupole	22 - 55	7.5
"slim" quadrupole	behind the quadrupole	2÷4 - 9	1.8

In Table IV total efficiency and the corresponding covered electron angles are reported for the different quadrupoles. We want to point out that only in the Panofsky quadrupole case the whole electron angular range from 2-4 mrad to 300 mrad is completely covered.

TABLE IV

Quadrupole	covered angles (mrad)	total efficiency (%)
Standard	2÷4 - 10 / 22 - 300	5.5 + 17 = 22.5
Panofsky	2÷4 - 300	10 + 17 = 27
"slim"	2÷4 - 9 / 22 - 300	1.8 + 17 = 18.8

$.1 < x_e < .95$

Effects of the real electron beam have been considered on the efficiency of the tagging device behind the quadrupole Q11 ; angular electron beam deviations have been studied up to 2 mrad and no significant deviation from the ideal case has been found. We think that the result on the angular deviation covers widely all possible combinations of the electron beam spread for $X_e \gtrsim 0.3$. So we conclude that one can expect no relevant deviations of the tagging efficiencies from the results given in Tables III and IV.

ACKNOWLEDGEMENT .

The author are grateful to P. Strolin for his critical reading of the manuscript and suggestions, to M. Preger for calculations and enlightening discussions on the LEP machine.

REFERENCES.

(1) - Physics with very high energy e^+e^- colliding beams, CERN 76-18 (1976).
(2) - J. Allaby et al., LEP Summer Study/1-7 (12/78).
(3) - B. Richter and P. Strolin, ECFA/LEP 48 (14/9/78).
(4) - J. Field, ECFA/LEP Summer Study/1-13 (10/78).
(5) - I. Peruzzi and M. Piccolo, ECFA/LEP Report, to be published.
(6) - "Blue Book".
(7) - C. Wyss, ECFA/LEP Report, to be published. A similar quadrupole has been built for the low-beta insertion of the ISR, see J. Billan et al., CERN 76-16 (1976).
(8) - See also Table I of the ref. (3). Systematic errors have been evaluated by M. Preger, like private communication.